Revisiting the $U_A(1)$ problems

D. Kekez*
Rudjer Bošković Institute, P.O.B. 1016, 10001 Zagreb, Croatia

D. Klabučar†
Physics Department, Faculty of Science, University of Zagreb,
Bijenička c. 32, Zagreb 10000, Croatia

M. D. Scadron‡
Physics Department, University of Arizona, Tucson, AZ 85721, USA

Abstract

We survey various $U_A(1)$ problems and attempt to resolve the two puzzles related to the eta mesons that have experimental verification. Specifically, we first explore the Goldstone structure of the η and η' mesons in the context of η–η' mixing using ideas based on QCD. Then we study the eta decays $\eta \to 3\pi^0$, $\eta' \to 3\pi^0$ and $\eta' \to \eta\pi\pi$. Finally we arrive at essentially the same picture in the dynamical scheme based on consistently coupled Schwinger-Dyson and Bethe-Salpeter integral equations. This chirally well-behaved bound-state approach clarifies the distinction between the usual axial-current decay constants and the $\gamma\gamma$ decay constants in the η–η' complex. Allowing for the effects of the SU(3) flavor symmetry breaking in the quark–antiquark annihilation, leads to the improved η–η' mass matrix.

11.30.Rd, 11.40.-q, 11.40.Ha, 11.10.St

Typeset using REVTEX

*kekez@lei.irb.hr

†klabucar@phy.hr

‡scadron@physics.arizona.edu

I. INTRODUCTION

Various statements of "$U_A(1)$ problems" related to the eta mesons and their possible resolutions have appeared in the literature now for almost three decades. Considerations of the eta $U_A(1)$ vacuum Ward identity were discussed by Glashow [1], Weinberg [2], Crewther [3] and collaborators. The $U_A(1)$ axial current and its anomalous addition were studied by Kogut and Susskind [4]. Semiclassical instantons with topological winding number were used by 't Hooft [5]. Lastly, the large N_c limit together with the θ vacuum were explored by Witten [6]. All of the above notions were invoked to resolve the $U_A(1)$ problem. These above $U_A(1)$ problems have recently been rekindled by 't Hooft in his text [7].

We prefer to focus on two $U_A(1)$-type problems that have empirical resolutions and which also have a theoretical basis:

1. Goldstone boson structure of the observed [8] $\eta(547)$ and $\eta'(958)$ mesons via η–η' mixing in the context of QCD.

2. Observed eta hadronic decay rates:

   (a) $\Gamma(\eta \to 3\pi^0) = 380 \pm 36$ eV [8] appears large since it should vanish by the Sutherland theorem [9], or be a factor of two smaller in the context of chiral perturbation theory [10].

   (b) $\Gamma(\eta' \to 3\pi^0) = 313 \pm 58$ eV [8] appears relatively suppressed because $\eta' \to 3\pi^0$ phase space is six times larger than for $\eta \to 3\pi^0$.

   (c) $\Gamma(\eta' \to \eta\pi\pi) = 131 \pm 8$ keV [8] is a strong decay, whereas the smaller 3π decays in 2a, 2b above change isospin by one unit and are non-strong decays proceeding through the quark mass difference $m_d - m_u$.

   (d) We invoke the $\Delta I = 1$ $u_3 = \overline{q}\lambda_3 q$ Coleman-Glashow (CG) [11] quark tadpole to support the current-current Sutherland [9] suppression of the $\eta \to 3\pi$ decay rates. The CG tadpole also explains all 13 hadron (P, V, B, D) SU(2) mass splittings [11,12]. Then we use PCAC Consistency [13] to compute the η, $\eta' \to 3\pi^0$ decay rates in 2a, 2b above.

The above problems are analyzed in Secs. II and III primarily on the basis of the input from meson phenomenology. However, the underlying notions of the quark model are also crucial in this analysis. Therefore, in Sec. IV we show the consistency of some of the results of Secs. II and III with a sophisticated quark model which has strong and clear connections with the fundamental theory – QCD. It is based on the so-called coupled Schwinger-Dyson (SD) and Bethe-Salpeter (BS) approach in which one, by solving the SD equation for dressed quark propagators of various flavors, explicitly constructs constituent quarks. They in turn build $q\bar{q}$ meson bound states which are solutions of the BS equation employing the dressed quark propagator obtained as the solution of the SD equation. If the SD and BS equations are so coupled in a consistent approximation, the light pseudoscalar mesons are simultaneously the $q\bar{q}$ bound states and the (quasi) Goldstone bosons of dynamical chiral symmetry breaking (DχSB). The resulting relativistically covariant constituent quark model (such as the variant of Ref. [14]) is consistent with current algebra because it incorporates the correct chiral symmetry behavior thanks to DχSB obtained in an, essentially, Nambu–Jona-Lasinio fashion, but the former model interaction is less schematic. In Refs. [14–19] for example, it is combined nonperturbative and perturbative gluon exchange; the effective propagator function is the sum of the known perturbative QCD contribution and the modeled nonperturbative component. For details, we refer to Refs. [14–18], while here we just note that the momentum-dependent dynamically generated quark mass functions $\mathcal{M}_f(q^2)$ (i.e., the quark propagator SD solutions for quark flavors f) illustrate well how the coupled SD-BS approach provides a modern constituent model which is consistent with perturbative and nonperturbative QCD. For example, the perturbative QCD part of the gluon propagator leads to the deep Euclidean behaviors of quark propagators (for all flavors) consistent with the asymptotic freedom of QCD [17]. However, what is important in the present paper, is the behavior of the same mass functions $\mathcal{M}_f(q^2)$ for low momenta [$q^2 = 0$ to $-q^2 \approx (400\,\mathrm{MeV})^2$], where $\mathcal{M}_f(q^2)$ (due to DχSB) have values consistent with typical values of the constituent mass parameter in constituent quark models. For the (isosymmetric) u- and d-quarks, our concrete model choice [14] gives us $\mathcal{M}_{u,d}(0) = 356$ MeV in the chiral limit (i.e., with vanishing $\widetilde{m}_{u,d}$, the explicit chiral symmetry breaking bare mass term in the quark propagator SD equation, resulting in vanishing pion mass eigenvalue, $m_\pi = 0$, in the BS equation), and $\mathcal{M}_{u,d}(0) = 375$ MeV [just 5% above $\mathcal{M}_{u,d}(0)$ in the chiral limit] with the explicit chiral symmetry breaking bare mass $\widetilde{m}_{u,d} = 3.1$ MeV, leading to a realistically light pion, $m_\pi = 140.4$ MeV. Similarly, for the s quark, $\mathcal{M}_s(0) = 610$ MeV. The simple-minded constituent mass parameters, denoted below by $\hat{m}$ in the case of the isosymmetric u and d quarks, and by m_s in the case of the s quarks, have therefore close analogues in the coupled SD-BS approach which explicitly incorporates some crucial features of QCD, notably DχSB.

II. GOLDSTONE STRUCTURE OF ETA MESONS

To resolve $\mathrm{U}_A(1)$ problem one, we invoke the U(3) pseudoscalar nonet structure ($\vec{\pi}, K, \eta, \eta'$) along with the Gell-Mann-Okubo mass formula $m_\pi^2 + 3m_{\eta_8}^2 = 4m_K^2$, requiring an octet eta mass $m_{\eta_8} \approx 567$ MeV. While this η_8 mass is presumed to vanish in the SU(3) $\times$ SU(3) chiral limit (CL), the companion singlet η_0 mass is not expected to vanish in the CL. Using the standard relation mixing η, η' to η_8, η_0 away from the CL one knows

$$m_{\eta_8}^2 + m_{\eta_0}^2 = m_\eta^2 + m_{\eta'}^2 \approx 1.22\ \mathrm{GeV}^2, \quad \text{or} \quad m_{\eta_0} \approx 947\ \mathrm{MeV} \tag{1}$$

for masses $\eta(547)$, $\eta'(958)$, $\eta_8(567)$.

Alternatively one can work in a nonstrange (NS)–strange (S) mixing basis which is more suitable for quark model considerations. Then one finds

$$m_{\eta_{NS}}^2 + m_{\eta_S}^2 = m_\eta^2 + m_{\eta'}^2 \approx 1.22\ \mathrm{GeV}^2, \tag{2}$$

along with the mixing relations

$$|\eta\rangle = \cos\phi\,|\eta_{NS}\rangle - \sin\phi\,|\eta_S\rangle \tag{3a}$$

$$|\eta'\rangle = \sin\phi\,|\eta_{NS}\rangle + \cos\phi\,|\eta_S\rangle\,. \tag{3b}$$

Clearly (2) follows from (3) given $\langle\eta'|\eta\rangle = 0$. The more familiar singlet-octet η–η' mixing angle θ defined in an analogous manner as in Eqs. (3) is geometrically related to ϕ above as [20] $\theta = \phi - \arctan\sqrt{2}$, with the latter angle 54.7°. World η–η' mixing angle data in 1989 led to [21]

$$\phi = 41^\circ \pm 2^\circ \qquad \text{or} \qquad \theta = -14^\circ \pm 2^\circ . \tag{4}$$

A more recent detailed analysis [22] based on 1996 data for decays tensor to pseudoscalar $T \to PP$, radiative vector to pseudoscalar (or vice versa) $V \to P\gamma$, $P \to V\gamma$, double radiative decays $\eta \to \gamma\gamma$, $\eta' \to \gamma\gamma$, and $J/\psi \to VP$ decays (14 such decays) leads to the empirical η–η' mixing angles

$$\phi = 43^\circ \pm 5^\circ \qquad \text{or} \qquad \phi = 42^\circ \pm 3^\circ \tag{5}$$

found respectively from observed branching ratios, $B(a_2 \to \eta\pi/K\overline{K}) = 2.96 \pm 0.53$, $B(a_2 \to \eta'\pi/\eta\pi) = 0.037 \pm 0.007$, in complete agreement with (4). The η–η' mixing angles in (4) or (5) (for 4 of 14 determinations) depend on the constituent quark mass ratio $m_s/\hat{m} \approx 1.45$, as already found from baryon magnetic moments [23], meson charge radii [24] and $K^* \to K\gamma$ decays [25]. ($\hat{m}$ denotes the isosymmetric average mass $m_{u,d}$.)

As for a theoretical determination of the η–η' mixing angle ϕ or $\theta = \phi - 54.7^\circ$, we follow the path of Refs. [20]. The contribution of the gluon axial anomaly to the singlet η_0 mass is essentially just parameterized and not really calculated, but some useful information can be obtained from the isoscalar $q\bar{q}$ annihilation graphs of which the "diamond" one in Fig. 1 is just the simplest example. That is, we can take Fig. 1 in the nonperturbative sense, where the two-gluon intermediate "states" represent any even number of gluons when forming a C$^+$ pseudoscalar $\overline{q}q$ meson [23], and where quarks, gluons and vertices can be dressed nonperturbatively, and possibly include gluon configurations such as instantons. Factorization of the quark propagators in Fig. 1 characterized by the ratio $X \approx \hat{m}/m_s$ leads to the pseudoscalar mass matrix in the NS–S basis [20]

$$\begin{pmatrix} m_\pi^2 + 2\beta & \sqrt{2}\beta X \\ \sqrt{2}\beta X & 2m_K^2 - m_\pi^2 + \beta X^2 \end{pmatrix} \to \begin{pmatrix} m_\eta^2 & 0 \\ 0 & m_{\eta'}^2 \end{pmatrix} , \tag{6}$$

where β denotes the total annihilation strength of the pseudoscalar $q\bar{q}$ for the *light* flavors $f = u, d$, whereas it is assumed attenuated by a factor X when a $s\bar{s}$ pseudoscalar appears. (The mass matrix in the η_8-η_0 basis reveals that in the $X \to 1$ limit, the CL-nonvanishing singlet η_0 mass is given by 3β.) The two parameters on the left-hand-side (LHS) of (6), β and X, are determined by the two diagonalized η and η' masses on the RHS of (6). The trace and determinant of the matrices in (6) then fix β and X to be [20]

$$\beta = \frac{(m_{\eta'}^2 - m_\pi^2)(m_\eta^2 - m_\pi^2)}{4(m_K^2 - m_\pi^2)} \approx 0.28 \text{ GeV}^2 \quad , \qquad X \approx 0.78 \ , \tag{7}$$

with the latter value suggesting a constituent quark mass ratio $X^{-1} \sim m_s/\hat{m} \sim 1.3$, near the values in Refs. [21–25], $m_s/\hat{m} \approx 1.45$.

This fitted nonperturbative scale of β in (7) depends only on the gross features of QCD. If instead one treats the QCD graph of Fig. 1 in the perturbative sense of literally two gluons exchanged, then one obtains [26] only $\beta_{2g} \sim 0.09$ GeV^2, which is about 1/3 of the needed scale of β found in (7). (This indicates that just the perturbative "diamond" graph can hardly represent even the roughest approximation to the effect of the gluon axial anomaly operator $\epsilon^{\alpha\beta\mu\nu}G^a_{\alpha\beta}G^a_{\mu\nu}$.) The above fitted quark annihilation (nonperturbative) scale β in (7) can be converted to the NS–S η–η' mixing angle ϕ in (3) from the alternative mixing relation $\tan 2\phi = 2\sqrt{2}\beta X(m^2_{\eta_S} - m^2_{\eta_{NS}})^{-1} \approx 9.2$ to [20]

$$\phi = \arctan\left[\frac{(m^2_{\eta'} - 2m^2_K + m^2_\pi)(m^2_\eta - m^2_\pi)}{(2m^2_K - m^2_\pi - m^2_\eta)(m^2_{\eta'} - m^2_\pi)}\right]^{1/2} \approx 41.9^\circ \ . \tag{8}$$

This kinematical QCD mixing angle (8) or $\theta = \phi - 54.7^\circ \approx -12.8^\circ$ has dynamical analogs [16], namely the coupled SD-BS approach mentioned in the Introduction and used in Sec. IV below. Since this predicted η–η' mixing angle in (8) is compatible with the empirical values in (4) and (5), we use (8) in the mixing angle relations (3) to infer the nonstrange and strange η masses,

$$m^2_{\eta_{NS}} = \cos^2\phi\ m^2_\eta + \sin^2\phi\ m^2_{\eta'} \approx (758\ \text{MeV})^2 \tag{9a}$$

$$m^2_{\eta_S} = \sin^2\phi\ m^2_\eta + \cos^2\phi\ m^2_{\eta'} \approx (801\ \text{MeV})^2 \ . \tag{9b}$$

Thus it is clear that the true physical masses $\eta(547)$ and $\eta'(958)$ are respectively much closer to the Nambu-Goldstone (NG) octet $\eta_8(567)$ and the non-NG singlet $\eta_0(947)$ configurations than to the nonstrange $\eta_{NS}(758)$ and strange $\eta_S(801)$ configurations inferred in Eqs. (9). However, the mean η–η' mass $(548 + 958)/2 \approx 753$ MeV is quite near the nonstrange $\eta_{NS}(758)$. But since $\eta_8(567)$ appears far from the NG massless limit we must ask: how close is $\eta_0(947)$ to the chiral-limiting nonvanishing singlet η mass?

To answer this latter question, return to Fig. 1 and the quark annihilation strength $\beta \approx 0.28\ \text{GeV}^2$ in Eq. (7). These $\bar{q}q$ states presumably hadronize into the $\mathrm{U}_A(1)$ singlet state $|\eta_0\rangle = |\bar{u}u + \bar{d}d + \bar{s}s\rangle/\sqrt{3}$, for effective squared mass in the SU(3) limit with β remaining unchanged [26]:

$$m^2_{\eta_0} = 3\beta \approx (917\ \text{MeV})^2. \tag{10}$$

This latter CL η_0 mass in (10) is only 3% shy of the exact chiral-broken $\eta_0(947)$ mass found in Eq. (1). (Such a 3% CL reduction also holds for the pion decay constant $f_\pi \approx 93$ MeV $\to 90$ MeV [27] and for $f_+(0) = 1 \to 0.97$ [28], the K–π K_{l3} form factor.)

Thus this η–η' mixing resolution of the first $\mathrm{U}_A(1)$ problem is that the physical $\eta(547)$ is 97% of the chiral-broken NG boson $\eta_8(567)$. Also the mixing-induced CL singlet mass of 917 MeV in (10) is 97% of the chiral-broken singlet $\eta_0(947)$ in (1), which in turn is 99% of the physical η' mass $\eta'(958)$. This speaks to Weinberg's question [2] as to why there is no isoscalar, pseudoscalar Goldstone boson (with mass less than about $\sqrt{3}m_\pi \sim 240$ MeV), associated with the spontaneous breakdown of the axial $\mathrm{U}_A(1)$ symmetry.

III. HADRONIC ETA DECAYS AND THE $\mathrm{U}_A(1)$ PROBLEM

As for the second $\mathrm{U}_A(1)$ problem, Weinberg in [2] correctly identified the rapidly varying η and π^0 poles for $\eta \to 3\pi^0$ decay. However, one must also fold in the PCAC consistency approach of Refs. [13,29] leading to the $\eta \to 3\pi^0$ amplitude magnitude with $f_\pi \approx 93$ MeV,

$$\left|\left\langle 3\pi^0\right| H_{\text{em}}\left|\eta\right\rangle\right| \quad = \quad (3/2f^2_\pi)\left|\left\langle \pi^0\right| H_{\text{em}}\left|\eta\right\rangle\right| + \mathcal{O}(m^2_\pi/m^2_\eta) \ . \tag{11a}$$

Here the factor of $3/f_\pi^2$ on the RHS of (11a) corresponds to the three successive double pion PCAC reductions, while the factor of 1/2 characterizes Weinberg's [2] rapidly varying η and π^0 pole terms. Also this $\Delta I = 1$ $\eta \to \pi$ non-strong transition in (11a) reduces to [12,13]

$$\left\langle \pi^0 \right| H_{\rm em} \left| \eta \right\rangle = \cos\phi \left\langle \pi^0 \right| u_3 \left| \eta_{NS} \right\rangle = \cos 42^\circ (\Delta m_K^2 - \Delta m_\pi^2) \approx -3900\,\mathrm{MeV}^2. \qquad (11b)$$

In (11b) we have invoked the CG $u_3 = \overline{q}\lambda_3 q$ quark tadpole (which is known [11,12] to explain all P, V, B, D hadron SU(2) electromagnetic (em) mass splittings) using the SU(3) form $\langle \pi^0 | u_3 | \eta_{NS} \rangle = \Delta m_K^2 - \Delta m_\pi^2 \approx -0.0052$ GeV^2, where $\Delta m_K^2 = m_{K^+}^2 - m_{K^0}^2$, etc. Also in (11b) we have again invoked the η–η' mixing relations (3a) with mixing angle predicted by (8).

Substituting (11b) into (11a), one obtains the $\eta \to 3\pi^0$ amplitude

$$\left| \left\langle 3\pi^0 \right| H_{\rm em} \left| \eta \right\rangle \right| = (3/2f_\pi^2) \left| \left\langle \pi^0 \right| H_{\rm em} \left| \eta \right\rangle \right| \approx 0.68 \quad . \qquad (12a)$$

As for the experimental $\eta_{3\pi^0}$ decay amplitude, taking a constant matrix element (12a) integrated over the Dalitz plot, one predicts an $\eta \to 3\pi^0$ decay rate

$$\Gamma(\eta_{3\pi^0}) = (816 \text{ eV}) \left| \left\langle 3\pi^0 \right| H_{\rm em} \left| \eta \right\rangle \right|^2 \approx 377 \text{ eV} \quad . \qquad (12b)$$

The latter almost perfectly matches the 1998 PDG [8] rate of 380 ± 36 eV at the central value.

Alternatively we can extract the effective constant 3-body matrix elements A_a, A_b, A_c from data [8]

$$\Gamma(\eta \to 3\pi^0) \approx 0.82 \; |A_a|^2 \, keV \approx 0.38 \text{ keV}, \qquad (13a)$$

$$\Gamma(\eta' \to 3\pi^0) \approx 5.58 \; |A_b|^2 \, keV \approx 0.31 \text{ keV}, \qquad (13b)$$

$$\Gamma(\eta' \to \eta\pi^0\pi^0) \approx 1.06 \; |A_c|^2 \, keV \approx 42 \text{ keV}, \qquad (13c)$$

leading to the dimensionless 3-body amplitudes

$$|A_a| \approx 0.68, \quad |A_b| \approx 0.24, \quad |A_c| \approx 6.3. \qquad (13d)$$

Note that the PCAC amplitude for $\langle 3\pi^0 | H_{em} | \eta \rangle$ in (12a) recovers the observed $\eta \to 3\pi^0$ rate in (12b) or equivalently the constant *Dalitz* plot amplitude forms in (13) give $|A_a| \approx 0.68$ which was earlier used to predict the $\eta \to 3\pi^0$ rate in Eqs. (12).

This consistency pattern can also be applied to $\eta' \to 3\pi^0$ decay, presumably dominated by [30] $\eta' \to \eta\pi^0\pi^0$ followed by an em transition $\langle \pi^0 | H_{em} | \eta \rangle$:

$$\left| \left\langle 3\pi^0 \right| H_{\rm em} \left| \eta' \right\rangle \right| = 3 \left| \left\langle \pi^0 \right| H_{\rm em} \left| \eta \right\rangle \langle \pi^0\pi^0\eta | \eta' \rangle \right| (m_\eta^2 - m_\pi^2)^{-1}$$

$$\approx 3(3900 \text{ MeV}^2)(6.3)(281000 \text{ MeV}^2)^{-1} \approx 0.26. \qquad (14a)$$

In (14a) we have again used the em scale (11b) (three times), the η propagator on the π^0 mass shell and the constant amplitude $|A_c| \approx 6.3$ in (13d). The result 0.26 is near the constant amplitude $|A_b| \approx 0.24$ in (13d), or equivalently the $\eta'_{3\pi}$ decay rate is predicted to be

$$\Gamma(\eta' \to 3\pi^0) \approx 5.58 \left| \left\langle 3\pi^0 \right| H_{\rm em} \left| \eta' \right\rangle \right|^2 \text{ keV} \approx 377 \text{ eV}, \qquad (14b)$$

near data [8] 313 ± 58 eV.

Finally we consider the strong decays $\eta' \to \eta\pi\pi$, with the charged to neutral pion branching ratio being [8] about 2, as expected via SU(2) symmetry. At first these decays were thought to be controlling the η–η' mixing angle. Now, however, one begins by assuming an η–η' mixing angle [such as $\phi \approx 42^\circ$ or $\theta \approx -13^\circ$ found earlier in Eqs. (4, 5, 8)] , and then attempts to explain the observed $\eta' \to \eta\pi\pi$ rate given in Sec. I.

To this end Singh and Pasupathy in Ref. [31] studied the $\delta = a_0(983)$ scalar meson pole amplitude in $\eta' \to \delta\pi$, $\delta \to \eta\pi$. Later Deshpande and Truong in [31] also included a scalar meson σ pole in this analysis with $\eta' \to \eta\sigma$, $\sigma \to \pi\pi$. These second authors in [31] justified introducing this latter σ in order to mask a soft-pion Adler zero which would drastically alter the $\pi\pi$ phase space. In fact the $\eta' \to \eta\pi^0\pi^0$ data shows only a small deviation from phase space, with linear amplitude $A(1+\alpha y)$ now requiring [8] $\alpha = -0.058 \pm 0.013$, and $\alpha = -0.08 \pm 0.03$ for $\eta' \to \eta\pi^+\pi^-$ decay.

Keeping only these two δ and σ pole terms, we slightly modify Refs. [31] and write this combined $\eta' \to \eta\pi^+\pi^-$ amplitude magnitude as

$$A = \left|A(\eta' \to \eta\pi^+\pi^-)\right| \approx \left|\frac{g_{\delta\eta\pi}g_{\eta'\delta\pi}}{m_\delta^2 - u - im_\delta\Gamma_\delta} + \frac{g_{\sigma\pi\pi}g_{\eta'\eta\sigma}}{m_\sigma^2 - s - im_\sigma\Gamma_\sigma}\right| . \tag{15}$$

Here the combined δ and σ pole amplitudes have the same structure as in Ref. [31] except we always (rather than partially) keep the non-narrow widths [8] $\Gamma_\delta \sim 100$ MeV and $\Gamma_\sigma \sim 700$ MeV [8,32]. Also to estimate the pole denominators in (15), we follow Ref. [31] and take $m_\delta^2 - u \approx 2m_{\eta'}E_1 \approx 2m_{\eta'}(m_{\eta'} - m_\eta)$ in the η' rest frame with $p_\pi \approx p_{\pi'} \approx 0$ soft and $s = [6.77 - 2.4y]\, m_\pi^2$.

Finally we choose the nonstrange σ mass from the recent data analysis of Ref. [33]:

$$m_\sigma = 400 \text{ to } 900 \text{ MeV} , \qquad \text{mean mass } m_\sigma \approx 650 \text{ MeV} . \tag{16}$$

This is near ε (700) used in [31] and is supported by the 1998 PDG tables [8]. Moreover a $\sigma(650)$ is generated from linear σ model (LσM) dynamics [34] with LσM coupling constants using the mixing relations (3):

$$g_{\delta\eta\pi} = \cos\phi\, g_{\delta\eta_{NS}\pi} = \cos\phi \left(\frac{m_\delta^2 - m_{\eta_{NS}}^2}{2f_\pi}\right) \approx 1.56 \text{ GeV}, \tag{17a}$$

$$g_{\eta'\delta\pi} = \sin\phi\, g_{\delta\eta_{NS}\pi} = \sin\phi \left(\frac{m_\delta^2 - m_{\eta_{NS}}^2}{2f_\pi}\right) \approx 1.40 \text{ GeV}, \tag{17b}$$

$$g_{\sigma\pi\pi} = m_{\sigma_{NS}}^2/2f_\pi \approx 2.27 \text{ GeV}, \tag{17c}$$

$$g_{\eta'\eta\sigma} = \cos\phi \sin\phi\, g_{\sigma\pi\pi} \approx 1.13 \text{ GeV} . \tag{17d}$$

Note that $g_{\delta\eta_{NS}\pi} = g_{\sigma\pi\pi}$ in the chiral limit and also that the η–η' mixing angle used ($\phi = 41.9^\circ$) is as found from Eq. (8).

Substituting the above numerical values back into (15) leads to the $\eta' \to \eta\pi^+\pi^-$ amplitude magnitude

$$|A| \approx \left|\frac{2.20}{0.79 - i0.10} + \frac{2.57}{0.29 - i0.46}\right| \approx 6.64 . \tag{18}$$

This LσM prediction in (18) should be compared with the original estimates in [31] of $|A| \approx 8.5$, $\alpha \approx -0.012$. Also, $|A| \approx 6.64$ in (18) is near $|A_c| \approx 6.3$ in (13d) assuming a constant matrix element and isospin invariance. Lastly accounting for the $\eta' \to \eta\pi^0\pi^0$ as well as the $\eta' \to \eta\pi^+\pi^-$ amplitude, and folding in the slight Dalitz plot slope we predict the total decay rate (for the average slope $\alpha \approx -0.07$):

$$\Gamma(\eta' \to \eta\pi\pi) = 3\,|A|^2\,(1 + 0.24\alpha + 0.27\alpha^2)\ \text{keV} \tag{19a}$$

$$\approx 130\ \text{keV}\ . \tag{19b}$$

This prediction (19b) is in very good agreement with present data (131 ± 8 keV) as given in Sec. I.

We differ from Ref. [31] primarily in that we use the LσM meson-meson couplings in Eqs. (17). An extraction of the $\delta\eta\pi$ coupling from the width of $\Gamma(\delta\eta\pi) \sim 100$ MeV [35] gives for $q = 321$ MeV:

$$\Gamma(\delta\eta\pi) = \frac{q\,|2g_{\delta\eta\pi}|^2}{8\pi m_\delta^2}\ ,\ \text{or}\quad |g_{\delta\eta\pi}| \sim 1.38\ \text{GeV}\ . \tag{20}$$

The latter coupling in (20) is reasonably near the LσM coupling 1.56 GeV in (17a).

IV. CONSISTENCY WITH DYNAMICAL CALCULATIONS

As pointed out in the Introduction and Sec. II, there is a dynamical approach to the question of the Goldstone boson structure of the mixed $\eta(547)$ and $\eta'(958)$ mesons [16], namely the coupled SD-BS approach incorporating some crucial features of QCD, which leads to the similar conclusions on the mixing angle and masses as the analysis in Sec. II. Before addressing its mass matrix, let us see what this approach tells us about the mixing angle that can be inferred from $\gamma\gamma$ decays. Since the SD-BS approach incorporates the correct chiral symmetry behavior thanks to DχSB and is consistent with current algebra, it reproduces (when care is taken to preserve the vector Ward-Takahashi identity of QED) the Abelian axial anomaly results, which are otherwise notoriously difficult to reproduce in bound-state approaches, as discussed in Ref. [17]. This gives particular weight to the constraints placed on the mixing angle θ by the SD-BS results on $\gamma\gamma$ decays of pseudoscalars.

A. $\gamma\gamma$ decays of the bound-state π^0, η, η'

We express the SU(3) pseudoscalar states π^0, η_8 and η_0 through the quark basis states $|f\bar{f}\rangle$ by

$$|P\rangle = \sum_f \left(\frac{\lambda^P}{\sqrt{2}}\right)_{ff} |f\bar{f}\rangle\ , \qquad (f = u, d, s)\ , \tag{21}$$

where $P = \pi^0, \eta_8, \eta_0$ simultaneously have the meaning of the respective indices $j = 3, 8, 0$ on the SU(3) Gell-Mann matrices $\lambda^j\,(j = 1, ..., 8)$ and on $\lambda^0 \equiv (\sqrt{2/3})\mathbf{1}_3$. This picks out the diagonal $\lambda^3, \lambda^8, \lambda^0$ in Eq. (21). For future convenience we write the $P(p) \to \gamma(k)\gamma(k')$ amplitudes as

$$T_P(k^2,k'^2) = \sum_f \left(\frac{\lambda^P}{\sqrt{2}}\right)_{ff} Q_f^2 \, \widetilde{T}_{f\bar{f}}(k^2,k'^2)\,, \tag{22}$$

where $\widetilde{T}_{f\bar{f}}(k^2,k'^2) \equiv T_{f\bar{f}}(k^2,k'^2)/Q_f^2$ are the "reduced" two-photon amplitudes obtained by removing the squared charge factors Q_f^2 from $T_{f\bar{f}}$, the $\gamma\gamma$ amplitude of the pseudoscalar quark-antiquark bound state of the hidden flavor $f\bar{f}$.

The decay amplitudes (into real photons, $k^2 = k'^2 = 0$) of the physical states η and η', are given in terms of the predicted [16] $\gamma\gamma$ decay amplitudes of the SU(3) states η_8 and η_0 as

$$T_\eta(0,0) = \cos\theta \, T_{\eta_8}(0,0) - \sin\theta \, T_{\eta_0}(0,0)\ , \tag{23}$$

$$T_{\eta'}(0,0) = \sin\theta \, T_{\eta_8}(0,0) + \cos\theta \, T_{\eta_0}(0,0)\ . \tag{24}$$

The best fit to the experimental $\gamma\gamma$ decay amplitudes was found in Ref. [16] for $\theta = -12^\circ$ for the concrete SD-BS model and parameters [14] adopted there. In order to show that in the SD-BS approach $\gamma\gamma$ decays imply θ somewhere in that ballpark (i.e., less negative than values favored by χPT) regardless of any model choice, and to be able to compare with other theoretical approaches which usually try to express $P \to \gamma\gamma$ amplitudes in terms of the leptonic (axial-current) decay constants f_P, let us start with the light u,d sector in the chiral (and soft) limit. There, the SD-BS approach yields analytically and exactly[1], and independently of the internal bound-state pion structure,

$$\widetilde{T}_{\pi^0}(0,0) \equiv \widetilde{T}_{u\bar{u}}(0,0) = \widetilde{T}_{d\bar{d}}(0,0) = \frac{N_c}{2\sqrt{2}\pi^2 f_\pi}\ , \tag{25}$$

$$T_{\pi^0}(0,0) = \frac{N_c}{2\sqrt{2}\pi^2 f_\pi} \sum_f \left(\frac{\lambda^3}{\sqrt{2}}\right)_{ff} Q_f^2 \ = \frac{1}{4\pi^2 f_\pi}\ . \tag{26}$$

Of course, the calculated [14,18,16] value of f_π does depend on the (modeling of the) internal pion structure, but the empirically successful axial-anomaly chiral-limit relation (26) does not.

The $\pi^0 \to \gamma\gamma$ decay amplitude for a possibly nonvanishing pion mass, can be used as a definition of pionic $\gamma\gamma$-decay constant $\bar{f}_\pi$ by demanding that this amplitude be written in the form of the massless, CL amplitude (26), but with $\bar{f}_\pi$ in place of f_π: $T_{\pi^0}(0,0) = 1/4\pi^2 \bar{f}_\pi$. Obviously, $\bar{f}_\pi = f_\pi$ in the CL, and $\bar{f}_\pi$ is a convenient way to re-express the $\gamma\gamma$ amplitude in the case of a nonvanishing pion mass, because the Veltman-Sutherland theorem, PCAC, and the empirical success of the chiral-limit anomaly result (26), guarantee that $\bar{f}_\pi \approx f_\pi$ always holds for any realistic description of the light u,d sector. For simplicity of discussion, we therefore use $\bar{f}_\pi = f_\pi$ *in this subsection*, as the Veltman-Sutherland theorem guarantees that this can be wrong only by several percent. Although the chiral limit formula (26) can be applied without reservations only to pions, it is customary to write the amplitudes for $\eta_8, \eta_0 \to \gamma\gamma$ in the same form as (26), defining thereby the $\gamma\gamma$-decay constants $\bar{f}_{\eta_8}$ and $\bar{f}_{\eta_0}$:

[1]The same holds [36,37] for the related process $\gamma \to \pi^+\pi^0\pi^-$.

$$T_{\eta_8}(0,0) \equiv \frac{N_c}{2\sqrt{2}\pi^2 \bar{f}_{\eta_8}} \sum_f \left(\frac{\lambda^8}{\sqrt{2}}\right)_{ff} Q_f^2 \;= \frac{f_\pi}{\bar{f}_{\eta_8}} \frac{T_{\pi^0}(0,0)}{\sqrt{3}}, \tag{27}$$

$$T_{\eta_0}(0,0) \equiv \frac{N_c}{2\sqrt{2}\pi^2 \bar{f}_{\eta_0}} \sum_f \left(\frac{\lambda^0}{\sqrt{2}}\right)_{ff} Q_f^2 \;= \frac{f_\pi}{\bar{f}_{\eta_0}} \frac{\sqrt{8}\, T_{\pi^0}(0,0)}{\sqrt{3}}. \tag{28}$$

As pointed out by [38], $\bar{f}_{\eta_8}$ and $\bar{f}_{\eta_0}$ are **not** *a priori* simply connected with the usual axial-current decay constants f_{η_8} and f_{η_0}, in contrast to $f_\pi \approx \bar{f}_\pi$. Expressing $T_{\eta_8}(0,0)$ and $T_{\eta_0}(0,0)$ through the $\gamma\gamma$-decay constants $\bar{f}_{\eta_8}$ and $\bar{f}_{\eta_0}$, yields the customary (see, e.g. [38]) forms for the η and η' decay widths:

$$\Gamma(\eta \to \gamma\gamma) = \frac{\alpha_{\rm em}^2}{64\pi^3} \frac{m_\eta^3}{3 f_\pi^2} \left[\frac{f_\pi}{\bar{f}_{\eta_8}} \cos\theta - \sqrt{8}\frac{f_\pi}{\bar{f}_{\eta_0}} \sin\theta\right]^2 \;, \tag{29}$$

$$\Gamma(\eta' \to \gamma\gamma) = \frac{\alpha_{\rm em}^2}{64\pi^3} \frac{m_{\eta'}^3}{3 f_\pi^2} \left[\frac{f_\pi}{\bar{f}_{\eta_8}} \sin\theta + \sqrt{8}\frac{f_\pi}{\bar{f}_{\eta_0}} \cos\theta\right]^2 \;. \tag{30}$$

The even more customary version of (29) and (30) in which the axial-current decay constants f_{η_8} and f_{η_0} appear in place of $\bar{f}_{\eta_8}$ and $\bar{f}_{\eta_0}$ requires a derivation where PCAC and soft meson technique are applied to the η–η' complex [39]. For the indeed light pion, these assumptions are impeccable (leading to $f_\pi = \bar{f}_\pi$), but not for the η–η' complex. For such a heavy particle as η' they are quite dubious. However, we do not need and do not use these assumptions since we *directly* calculated the η_8 and η_0 decay amplitudes, i.e., $\bar{f}_{\eta_8}$ and $\bar{f}_{\eta_0}$, just as the axial-current pseudoscalar decay constants f_{η_8} and f_{η_0} were calculated [16] independently of the $\gamma\gamma$ processes. In contrast to $f_\pi = \bar{f}_\pi$, f_{η_8} and $\bar{f}_{\eta_8}$ cannot be equated, as the difference between them was found to be quite important [16].

The precise values of $\bar{f}_{\eta_8}$ and $\bar{f}_{\eta_0}$ are model dependent, but $\bar{f}_{\eta_8} < \bar{f}_\pi \approx f_\pi$ holds in this approach[2] generally, i.e., independently of chosen model details, as long as the s-quark mass is realistically heavier than the u, d-quark masses. To see this, let us start by noting that $\bar{f}_{\eta_8} < f_\pi$ is equivalent to $T_{\eta_8}(0,0) > T_{\pi^0}(0,0)/\sqrt{3}$, and since we can re-write Eq. (22) for η_8 as

$$T_{\eta_8}(0,0) = \frac{T_{\pi^0}(0,0)}{\sqrt{3}} + \frac{1}{9}\frac{2}{\sqrt{6}}\left[\widetilde{T}_{d\bar{d}}(0,0) - \widetilde{T}_{s\bar{s}}(0,0)\right] \,, \tag{31}$$

the inequality $\bar{f}_{\eta_8} < f_\pi$ is in our approach simply the consequence of the fact that the ("reduced") $\gamma\gamma$-amplitude of the $s\bar{s}$-pseudoscalar bound state, $\widetilde{T}_{s\bar{s}}$, is smaller than the corresponding non-strange $\gamma\gamma$-amplitude $\widetilde{T}_{d\bar{d}}$ ($= \widetilde{T}_{u\bar{u}} = \widetilde{T}_{\pi^0}$ in the isosymmetric limit), for any realistic relationship between the non-strange and much larger strange quark masses. This

[2]This is different from chiral perturbation theory [40]. Nevertheless, for the *axial-current* decay constants our SD-BS approach gives [16] $f_{\eta_8} = 1.31 f_\pi$ and $f_{\eta_0} = 1.16 f_\pi$ which ultimately led us to the axial-current decay constants of the physical etas, $f_{\eta'} = 1.26 f_\pi$ and $f_\eta = 1.21 f_\pi$, which *is* in a good agreement with the result $f_\eta = 1.02 f_\pi (f_K/f_\pi)^{4/3}$ of chiral perturbation theory [41].

is the reason why in this approach one cannot fit well the experimental $\eta, \eta' \to \gamma\gamma$ widths with the mixing angle as negative as in chiral perturbation theory descriptions ($\theta \sim -20^\circ$), but rather with $\theta \sim -12^\circ$. This is easily understood, for example, with the help of Fig. 1. of Ball *et al.* [42], where the values of $\bar{f}_{\eta 8(0)}/f_\pi$ consistent with experiment are given as a function of the mixing angle θ. Their curve shows that values $\bar{f}_{\eta 8}/f_\pi < 1$ permit accurate reproduction of $\eta, \eta' \to \gamma\gamma$ widths only for θ-values less negative than -15°. [It does not matter that they in fact plotted $f_{\eta 8(0)}/f_\pi$ and not $\bar{f}_{\eta 8(0)}/f_\pi$. Namely, they used Eqs. (29)-(30) for comparison with the experimental $\gamma\gamma$-widths, just with $f_{\eta 8(0)}/f_\pi$ instead of $\bar{f}_{\eta 8(0)}/f_\pi$, so that the experimental constraints displayed in their Fig. 1 apply to whatever ratios are used in these expressions. One should also note that since in our approach $\bar{f}_{\eta 8}, \bar{f}_{\eta 0}$ and f_π are not free parameters but predicted quantities, the two widths $\eta, \eta' \to \gamma\gamma$ cannot be fitted *exactly* by adjusting just one parameter, θ. Rather, we fix θ by performing a χ^2 fit to the widths.] On the other hand, the more negative values $\theta \lesssim -20^\circ$ give good $\eta, \eta' \to \gamma\gamma$ widths in conjunction with the ratio $\bar{f}_{\eta 8}/f_\pi = f_{\eta 8}/f_\pi = 1.25$ obtained by [40] in χPT. However, the coupled SD-BS approach belongs among constituent quark approaches, and for them, considerably less negative angles, $\theta \approx -14^\circ \pm 2$ [21], are natural.

Ref. [16] showed that these bounds and estimates are very robust under SD-BS model variations and can be taken as model independent. For example, for chiral u, d quarks,

$$\bar{f}_{\eta 8} = \frac{3\, f_\pi}{5 - \frac{4\pi^2 \sqrt{2} f_\pi}{N_c} \widetilde{T}_{s\bar{s}}(0,0)}\,, \qquad \bar{f}_{\eta 0} = \frac{6\, f_\pi}{5 + \frac{2\pi^2 \sqrt{2} f_\pi}{N_c} \widetilde{T}_{s\bar{s}}(0,0)}\,, \tag{32}$$

leading to the bounds $\frac{3}{5} f_\pi < \bar{f}_{\eta 8} < f_\pi$ and $f_\pi < \bar{f}_{\eta 0} < \frac{6}{5} f_\pi$. Also, considerations based on the Goldberger-Trieman relation showed that $\widetilde{T}_{s\bar{s}}(0,0) < \widetilde{T}_{u\bar{u}}(0,0)$ is simply due to $f_{s\bar{s}} \sim f_\pi + 2(f_{K^+} - f_\pi) > f_\pi$ (where $f_{s\bar{s}}$ is the axial-current decay constant of the unphysical $s\bar{s}$ pseudoscalar bound state), and that a good estimate of the $\gamma\gamma$-amplitude ratio is the inverse ratio of the pertinent *constituent* quark masses: $\widetilde{T}_{s\bar{s}}(0,0)/\widetilde{T}_{u\bar{u}}(0,0) \approx \hat{m}/m_s$. Equations (32) then give the relations [reducing to $\bar{f}_{\eta 8} = f_\pi$ and $\bar{f}_{\eta 0} = f_\pi$ in the U(3) limit, just like Eqs. (32) themselves]

$$\bar{f}_{\eta 8} \approx \frac{3\, f_\pi}{5 - 2\, \hat{m}/m_s}\,, \qquad \bar{f}_{\eta 0} \approx \frac{6\, f_\pi}{5 + \hat{m}/m_s}\,, \tag{33}$$

obtained also by Ref. [43] using the simple quark loop model with constant constituent masses. These estimates are (for reasonable $\hat{m}/m_s$) close to what Ref. [16] calculated with a concrete SD-BS model choice [14], namely $\bar{f}_{\eta 0}/f_\pi = 1.067$ and $\bar{f}_{\eta 8}/f_\pi = 0.797$. For these concrete model values, $\eta, \eta' \to \gamma\gamma$ widths (29)-(30) fit the data best for $\theta = -12.0^\circ$.

B. Introducing X into the SD-BS mass matrix

For the very predictive SD-BS approach to be consistent, the above mixing angle extracted from $\eta, \eta' \to \gamma\gamma$ widths, should be close to the angle θ predicted by diagonalizing the η–η' mass matrix. In this subsection, it is given in the quark $f\bar{f}$ basis:

$$M^2 = \mathrm{diag}(M^2_{u\bar{u}}, M^2_{d\bar{d}}, M^2_{s\bar{s}}) + \beta \begin{bmatrix} 1 & 1 & 1 \\ 1 & 1 & 1 \\ 1 & 1 & 1 \end{bmatrix}\,. \tag{34}$$

As in Sec. II, 3β (called λ_η in Ref. [16]) is the contribution of the gluon axial anomaly to $m_{\eta_0}^2$, the squared mass of η_0. We denote by $M_{f\bar{f}'}$ the masses obtained as eigenvalues of the BS equations for $q\bar{q}$ pseudoscalars with the flavor content $f\bar{f}'$ ($f, f' = u, d, s$). However, since Ref. [16] had to employ a rainbow-ladder approximation (albeit the improved one of Ref. [14]), it could not calculate the gluon axial anomaly contribution 3β. It could only avoid the $\mathrm{U}_A(1)$-problem in the η–η' complex by *parameterizing* 3β, namely that part of the η_0 mass squared which remains nonvanishing in the CL. Because of the rainbow-ladder approximation (which does not contain even the simplest annihilation graph – Fig. 1), the $q\bar{q}$ pseudoscalar masses $M_{f\bar{f}'}$ *do not* contain any contribution from 3β, unlike the nonstrange and strange η masses $m_{\eta_{NS}}$ [in Eq. (9a)] and m_{η_S} [in Eq. (9b)], which do, and which must not be confused with $M_{u\bar{u}} = M_{d\bar{d}}$ and $M_{s\bar{s}}$. Since the flavor singlet gluon anomaly contribution 3β does not influence the masses m_π and m_K of the non-singlet pion and kaon, the realistic rainbow-ladder modeling aims directly at reproducing the empirical values of these masses: $M_{u\bar{u}} = M_{d\bar{d}} = m_\pi$ and $M_{u\bar{d}} = m_K$. In contrast, the masses of the physical etas, m_η and $m_{\eta'}$, must be obtained by diagonalizing the η_8-η_0 sub-matrix containing both $M_{f\bar{f}}$ and the gluon anomaly contribution to $m_{\eta_0}^2$.

Since the gluon anomaly contribution 3β vanishes in the large N_c limit as $1/N_c$, while all $M_{f\bar{f}'}$ vanish in CL, our $q\bar{q}$ bound-state pseudoscalar mesons behave in the $N_c \to \infty$ and chiral limits in agreement with QCD and χPT (e.g., see [41]): as the strict CL is approached for all three flavors, the SU(3) octet pseudoscalars *including* η become massless Goldstone bosons, whereas the chiral-limit-nonvanishing η'-mass 3β is of order $1/N_c$ since it is purely due to the gluon anomaly. If one lets $3\beta \to 0$ (as the gluon anomaly contribution behaves for $N_c \to \infty$), then for any quark masses and resulting $M_{f\bar{f}}$ masses, the "ideal" mixing ($\theta = -54.74^\circ$) takes place so that η consists of u, d quarks only and becomes degenerate with π, whereas η' is the pure $s\bar{s}$ pseudoscalar bound state with the mass $M_{s\bar{s}}$.

In Ref. [16], numerical calculations of the mass matrix were performed for the realistic chiral and SU(3) symmetry breaking, with the finite quark masses (and thus also the finite BS $q\bar{q}$ bound-state pseudoscalar masses $M_{f\bar{f}}$) fixed by the fit [14] to static properties of many mesons but excluding the η–η' complex. The mixing angle which diagonalizes the η_8-η_0 mass matrix thus depended in Ref. [16] only on the value of the additionally introduced "gluon anomaly parameter" 3β. Its preferred value turned out to be $3\beta = 1.165$ GeV^2=(1079 MeV)^2, leading to the mixing angle $\theta = -12.7^\circ$ [compatible with $\phi = 41.9^\circ$ in Eq. (8)] and acceptable $\eta \to \gamma\gamma$ and $\eta' \to \gamma\gamma$ decay amplitudes. Also, the η mass was then fitted to its experimental value, but such a high value of 3β inevitably resulted in a too high η' mass, above 1 GeV. (Conversely, lowering 3β aimed to reduce $m_{\eta'}$, would push θ close to -20°, making predictions for $\eta, \eta' \to \gamma\gamma$ intolerably bad.) However, unlike Eq. (6) in the present paper, it should be noted that Ref. [16] did not introduce into the mass matrix the "strangeness attenuation parameter" X which should suppress the nonperturbative quark $f\bar{f} \to f'\bar{f}'$ annihilation amplitude (illustrated by the "diamond" graph in Fig. 1) when f or f' are strange.

On the other hand, the influence of this suppression should be substantial, since $X \approx \hat{m}/m_s$ should be a reasonable estimate of it, and this nonstrange-to-strange *constituent* mass ratio in the considered variant of the SD-BS approach [16] is not far from X in Eq. (7) and from the mass ratios in Refs. [23–25], and is even closer to the mass ratios in the Refs. [22]. Namely, two of us found [16] it to be around $\mathcal{M}_u(0)/\mathcal{M}_s(0) = 0.615$ if the constituent mass was defined at the vanishing argument q^2 of the momentum-dependent SD mass function $\mathcal{M}_f(q^2)$.

We therefore introduce the suppression parameter X the same way as in the NS–S mass matrix (6), whereby the mass matrix in the $f\bar{f}$ basis becomes

$$M^2 = \mathrm{diag}(M^2_{u\bar{u}}, M^2_{d\bar{d}}, M^2_{s\bar{s}}) + \beta \begin{bmatrix} 1 & 1 & X \\ 1 & 1 & X \\ X & X & X^2 \end{bmatrix} . \tag{35}$$

In a very good approximation, Eq. (35) recovers (in the π^0–NS–S basis) Eq. (6) for the 2×2 η–η' subspace. This is because $M^2_{s\bar{s}}$ differs from $2m_K^2 - m_\pi^2$ only by a couple of percent, thanks to the good chiral behavior of the masses $M_{f\bar{f}'}$ calculated in SD-BS approach. (These $M^2_{f\bar{f}'}$ and the CL model values of f_π and quark condensate, satisfy Gell-Mann-Oakes-Renner relation to the first order in the explicit chiral symmetry breaking [15].) The SD-BS–predicted octet (quasi-)Goldstone masses $M_{f\bar{f}'}$ are known to be empirically successful in our concrete model choice [14], but the question is whether the SD-BS approach can also give some information on the X-parameter. If we treat *both* 3β and X as free parameters, we can of course fit both the η mass and the η' mass to their experimental values. For the model parameters as in Ref. [14] (for these parameters our independent calculation gives $m_\pi = M_{u\bar{u}} = 140.4$ MeV and $M_{s\bar{s}} = 721.4$ MeV), this happens at $3\beta = 0.753$ GeV^2 =(868 MeV)^2 and $X = 0.835$. However, the mixing angle then comes out as $\theta = -17.9°$, which is too negative to allow consistency of the empirically found two-photon decay amplitudes of η and η', with predictions of our SD-BS approach for the two-photon decay amplitudes of η_8 and η_0 [16].

Therefore, and also to avoid introducing another free parameter in addition to 3β, we take the path where the dynamical information from our SD-BS approach is used to estimate X. Namely, our $\gamma\gamma$ decay amplitudes $T_{f\bar{f}}$ can be taken as a serious guide for estimating the X-parameter instead of allowing it to be free. We did point out in Sec. II that the attempted treatment [26] of the gluon anomaly contribution through just the "diamond diagram" contribution to 3β, indicated that just this partial contribution is quite insufficient. This limits us to keeping 3β as a free parameter, but we can still suppose that this diagram can help us get the prediction of the strange-nonstrange *ratio* of the complete pertinent amplitudes $f\bar{f} \to f'\bar{f}'$ as follows. Our SD-BS modeling in Ref. [16] employs an infrared-enhanced gluon propagator [14,17] weighting the integrand strongly for low gluon momenta squared. Therefore, in analogy with Eq. (4.12) of Kogut and Susskind [4] (see also Refs. [44,45]), we can approximate the Fig. 1 amplitudes $f\bar{f} \to 2\text{gluons} \to f'\bar{f}'$, i.e., the contribution of the quark-gluon diamond graph to the element ff' of the 3×3 mass matrix, by the factorized form

$$\widetilde{T}_{f\bar{f}}(0,0)\, \mathcal{C}\, \widetilde{T}_{f'\bar{f}'}(0,0)\, . \tag{36}$$

In Eq. (36), the quantity $\mathcal{C}$ is given by the integral over two gluon propagators remaining after factoring out $\widetilde{T}_{f\bar{f}}(0,0)$ and $\widetilde{T}_{f'\bar{f}'}(0,0)$, the respective amplitudes for the transition of the $q\bar{q}$ pseudoscalar bound state for the quark flavor f and f' into two vector bosons, in this case into two gluons. The contribution of Fig. 1 is thereby expressed with the help of the (reduced) amplitudes $\widetilde{T}_{f\bar{f}}(0,0)$ we calculated for the transition of $q\bar{q}$ pseudoscalars to two real photons ($k^2 = k'^2 = 0$). Although $\mathcal{C}$ is in principle computable, all this unfortunately does not amount to determining $\beta, \beta X$ and βX^2 in Eq. (35) since the higher (four-gluon, six-gluon, ... , etc.) contributions are clearly lacking. We therefore must keep the total (light-)quark annihilation strength β as a free parameter. However, if we assume that the suppression of the diagrams with the strange quark in a loop is similar for all of them, Eq. (36) and the "diamond" diagram in Fig. 1 help us to at least estimate the parameter X as $X \approx \widetilde{T}_{s\bar{s}}(0,0)/\widetilde{T}_{u\bar{u}}(0,0)$. This is a natural way to build in the effects of the SU(3) flavor symmetry breaking in the $q\bar{q}$ annihilation graphs.

We get $X = 0.663$ from the two-photon amplitudes we obtained in the chosen SD-BS model [14]. This value of X agrees well with the other way of estimating X, namely the nonstrange-to-strange constituent mass ratio of Refs. [23–25]. With $X = 0.663$, requiring that the 2×2 matrix trace, $m_\eta^2 + m_{\eta'}^2$, be fitted to its empirical value, fixes the chiral-limiting nonvanishing singlet mass squared to $3\beta = 0.832$ GeV^2=(912 MeV)^2, just 0.5% below Eq. (10). The resulting mixing angle and η, η' masses are

$$\theta = -13.4^\circ\,, \qquad m_\eta = 588\,\mathrm{MeV}\,, \qquad m_{\eta'} = 933\,\mathrm{MeV}\,. \tag{37}$$

The above results of the SD-BS approach [16] are very satisfactory since they agree well with what was found in Sec. II by different methods. Let us close this section by exploring the stability of these results on model variations. Except the introduction of $3\beta (= \lambda_\eta)$, these SD-BS results were obtained without any other parameter fitting, with the model parameters resulting from the very broad previous fit [14], but actually giving us, in our independent calculation, a few percent too high results for m_π and m_K. To possibly improve, and in any case check the robustness of the consistency with Sec. II (and subsection IV.A) on variations of our model description, we therefore perform a refitting in the sector of u, d and s quarks, to reproduce exactly the average isotriplet pion mass $m_\pi = M_{u\bar{u}} = 137.3$ MeV and isodoublet kaon mass $m_K = 495.7$ MeV. As Table I shows, the changes are small, and lead to $\mathcal{M}_u(0)/\mathcal{M}_s(0) = 0.622$ and $X = \widetilde{T}_{s\bar{s}}(0,0)/\widetilde{T}_{u\bar{u}}(0,0) = 0.673$. Using this X to fit the sum of the squared η and η' masses to the empirical value, yields the column B in Table II, where we see a slight improvement in the η and η' masses with respect to the results (37), while the mixing angle is still acceptable, being less than 2° away from the angle favored in Sec. II.

If we treat X as the second free parameter (this procedure yields the column C of Table II) so that we are able to fit m_η and $m_{\eta'}$ precisely to their experimental values, we get $X = 0.805$, along with the mixing angle $\theta = -14.9^\circ$ and the chiral-limit-nonvanishing singlet mass $3\beta = 0.801$ GeV^2=(895 MeV)^2. This is noticeably closer to θ and 3β resulting from other procedures (where X is not a free parameter) than before the aforementioned $\pi^0 - K$ refitting to $m_\pi = 137.3$ MeV and $m_K = 495.7$ MeV.

Next, we note in the column D of Table II that the slightly improved fit to the masses also led to somewhat improved $\eta, \eta' \to \gamma\gamma$ widths when we extract from them $\theta = -12.8^\circ$, practically the same as Ref. [16] and the Sec. II result (8). All the three possibilities B, C, and D, do not differ too much from each other, and agree reasonably with the experimental masses and $\gamma\gamma$ widths given in column E as well as with the corresponding results of Sec. II. This contrasts with column A, which also contains the results of the new fit but with $X = 1$. Column A shows that when $X = 1$, a good description of the masses requires a θ

value too negative for a good description of the $\gamma\gamma$ widths in the SD-BS approach. Column A thus convinces us that it was precisely the lack of the strangeness attenuation factor X that prevented Ref. [16] from satisfactorily reproducing the η' mass when it successfully did so with the η mass and $\gamma\gamma$ widths.

V. CONCLUSION

In Sec. II we studied the first $U_A(1)$ problem associated with the Goldstone structure of $\eta(547)$ and $\eta'(958)$ mesons. Following a QCD gluon-mediated approach to η–η' particle mixing, we began by extracting an η–η' mixing angle $\phi \approx 42°$ in the NS–S basis or $\theta \approx -13°$ in the singlet-octet basis. This led to eta masses $\eta_8(567)$, $\eta_0(947)$ with chiral-limiting (CL) $\eta_0(917)$. Then the physical eta mass $\eta(547)$ is 97% of $\eta_8(567)$, while $\eta'(958)$ is 104% of the CL $\eta_0(917)$. Such a 3–4% CL suppression is likewise found for the pion decay constant $f_\pi \approx 93$ MeV $\to 90$ MeV and for the K_{l3} form factor $f_+(0) = 1 \to 0.96$–0.97.

Then in Sec. III we studied the second $U_A(1)$ problem associated with eta meson hadronic decay rates. The $\eta, \eta' \to 3\pi^0$ ($\Delta I = 1$) decay rates of 377 eV followed from PCAC Consistency. Also a (strong) decay rate of 130 keV for $\eta' \to \eta\pi\pi$ was obtained from δ and σ scalar meson poles combined with linear σ model couplings. These three rates are compatible with data finding [8] $\Gamma(\eta \to 3\pi^0) = 380 \pm 36$ eV, $\Gamma(\eta' \to 3\pi^0) = 313 \pm 58$ eV and $\Gamma(\eta' \to \eta\pi\pi) = 131 \pm 8$ keV.

Finally, in Sec. IV we showed the consistency of the above results with those obtained in a chirally well-behaved quark model which was explicitly constructed through DχSB, SD and BS equations. For example, described variations of our SD-BS approach lead to $\theta \approx -13° \pm 2°$ and to the corresponding CL η_0 mass $\sqrt{3\beta} = 912 \pm 18$ MeV. Successful reproduction of the Abelian axial anomaly amplitudes in the CL in this bound-state approach, gives particular weight to our conclusion that so far away from the CL as in the case of the η–η' complex, $\gamma\gamma$-decay constants $(\bar{f}_{\eta_8}, \bar{f}_{\eta_0})$ differ significantly from the usual axial-current decay constants (f_{η_8}, f_{η_0}). By allowing for the effects of the SU(3) flavor symmetry breaking also in $q\bar{q}$ annihilation graphs, we have improved the η–η' mass matrix with respect to the mass matrix in Ref. [16].

Acknowledgments: M. D. S. appreciates discussions with H. F. Jones, R. Delbourgo and V. Elias, and thanks the Univ. of Western Ontario for hospitality. D. Kl. and D. Ke. acknowledge the support of the Croatian Ministry of Science and Technology under the respective contract numbers 1–19–222 and 009802.

REFERENCES

[1] S. L. Glashow in "Hadrons and their interactions", Erice 1967, ed. A. Zichichi (Acad. Press, New York, 1968) p. 83; S. L. Glashow, R. Jackiw and S. S. Shei, Phys. Rev. **187**, 1916 (1969).

[2] S. Weinberg, Phys. Rev. D **11,** 3583 (1975).

[3] R. Crewther, Phys. Lett. B **70**, 349 (1977); Riv. Nuovo Cimento, **2**, 63 (1979); G. A. Christos, Phys. Repts. **116**, 251 (1984).

[4] J. Kogut and L. Susskind, Phys. Rev. D **10**, 3468 (1974); D **11**, 3594 (1975).

[5] G. 'tHooft, Phys. Rev. Lett. **37**, 8 (1976); Phys Rev. D**14**, 3432 (1976).

[6] E. Witten, Nucl. Phys. B **149**, 285 (1978); B **156**, 269 (1979); R. Weder, Phys. Lett. B **85**, 269 (1979).

[7] G. 'tHooft, "Under the Spell of the Gauge Principle", World Scientific, Singapore, 1994, pp. 191–193, 323–351.

[8] Particle Data Group, C. Caso et al., Eur. Phys. J. **3**, 1 (1998).

[9] D. A. Sutherland, Phys. Lett. **23**, 384 (1966).

[10] See e.g. Crystal Barrel Collab., C. Amsler et al., Nuovo Cimento A **107**, 2589 (1994).

[11] S. Coleman and S. L. Glashow, Phys. Rev. Lett. **6**, 423 (1961); Phys. Rev. **134**, B**671** (1964).

[12] S. A. Coon and M. D. Scadron, Phys. Rev. C**51**, 2923 (1995).

[13] S. R. Choudhury, R. E. Karlsen and M. D. Scadron, Int. Jour. Mod. Phys. A 11, 271 (1996).

[14] P. Jain and H. J. Munczek, Phys. Rev. D **48**, 5403 (1993).

[15] H. J. Munczek and P. Jain, Phys. Rev. D **46**, 438 (1992).

[16] D. Klabučar and D. Kekez, Phys. Rev. D **58**, 096003 (1998), hep-ph/9710206.

[17] D. Kekez, B. Bistrović and D. Klabučar, Int. J. Mod. Phys. A**14**, 161 (1999).

[18] D. Kekez and D. Klabučar, Phys. Lett. B **387**, 14 (1996).

[19] D. Kekez and D. Klabučar, Phys. Lett. B **457**, 359 (1999).

[20] H. F. Jones and M. D. Scadron, Nucl. Phys. B **155**, 409 (1979); M. D. Scadron, Phys. Rev. D**29**, 2076 (1984).

[21] A. Bramon and M. D. Scadron, Phys. Lett. B **234**, 346 (1990).

[22] A. Bramon, R. Escribano and M. D. Scadron, Phys. Lett. B **403**, 339 (1997); Eur. Phys. J. C**7**, 271 (1999).

[23] A. De Rújula, H. Georgi and S. Glashow, Phys. Rev. D **12**, 147 (1975).

[24] See e.g. C. Ayala and A. Bramon, Europhys. Lett. **4**, 777 (1987) and references therein.

[25] A. Bramon and M. D. Scadron, Phys. Rev. D **40**, 3779 (1989).

[26] A. Patrascioiu and M. D. Scadron, Phys. Rev. D **22**, 2054 (1980); R. Delbourgo and M. D. Scadron, ibid. D **28**, 2345 (1983); S. R. Choudhury and M. D. Scadron, Mod. Phys. Lett. A **1**, 535 (1986).

[27] M. D. Scadron, Rep. Prog. Phys. **44**, 213 (1981), see pp. 247, 268; S. A. Coon and M. D. Scadron, Phys. Rev. C **23**, 1150 (1981).

[28] L. F. Li and H. Pagels, Phys. Rev. D **5**, 1509 (1972); N. Paver and M. D. Scadron, ibid. D **30**, 1988 (1984).

[29] R. E. Karlsen and M. D. Scadron, Phys. Rev. D **45**, 4108 (1992).

[30] D. J. Gross, S. B. Treiman and F. Wilczek, Phys. Rev. D **19** , 2188 (1979).

[31] C. Singh and J. Pasupathy, Phys. Rev. Lett. **35**, 1193 (1975); N.G. Deshpande and T.N. Truong, Phys. Rev. Lett. **41**, 1579 (1978); A.H. Fariborz and J. Schechter, Phys. Rev. D **60**, 034002 (1999). For simplicity, we have neglected the small contact and $f_0(980) \to 2\pi$ amplitudes as in Fig. 2 of the third reference.
[32] S. Weinberg, Phys. Rev. Lett. **65**, 1177 (1990); M. D. Scadron, Mod. Phys. Lett. A **7**, 479 (1992).
[33] N. Tornqvist and M. Roos, Phys. Rev. Lett. **76**, 1575 (1996).
[34] R. Delbourgo and M. D. Scadron, Mod. Phys. Lett. A **10**, 251 (1995), hep-ph/9910242; M. D. Scadron, Phys. Rev. D **57**, 5307 (1998), hep-ph/9712425; M. D. Scadron, Eur. Phys. J. C **6**, 141 (1999), hep-ph/9710317.
[35] B. Armstrong et al., Z. Phys. C **52**, 389 (1991).
[36] R. Alkofer and C. D. Roberts, Phys. Lett. B **369**, 101 (1996).
[37] B. Bistrović and D. Klabučar, hep-ph/9912452.
[38] J. F. Donoghue, E. Golowich and B. R. Holstein, *Dynamics of the Standard Model* (Cambridge University Press 1992).
[39] G. R. Farrar and G. T. Gabagadze, Phys. Lett. B **397**, 104 (1997).
[40] J. F. Donoghue, B. R. Holstein and Y.-C. R. Lin, Phys. Rev. Lett. **55**, 2766 (1985).
[41] J. Gasser and H. Leutwyler, Nucl. Phys. B **250**, 465 (1985).
[42] P. Ball, J. M. Frère and M. Tytgat, Phys. Lett B **365**, 367 (1996).
[43] R. Delbourgo, D. Liu and M.D. Scadron, Int. J. Mod. Phys. A **14**, 4331 (1999).
[44] M. R. Frank and T. Meissner, Phys. Rev. C **57**, 345 (1998).
[45] L. v. Smekal, A. Mecke and R. Alkofer, hep-ph/9707210.

P	m_P	f_P	$T_P(0,0)$	$\mathcal{M}_q(0)$
π	0.1373	0.0931	0.257	0.374
K	0.4957	0.113		
$s\bar{s}$	0.7007	0.135	0.0815	0.601

TABLE I. The first column displays results of refitting π, K and $s\bar{s}$ masses ($m_{s\bar{s}} \equiv M_{s\bar{s}}$) obtained in the $q\bar{q}$ bound state SD-BS approach with the slightly changed explicit chiral symmetry breaking bare masses $\widetilde{m}_{u,d} = 2.965$ MeV and $\widetilde{m}_s = 69.25$ MeV. These π and $s\bar{s}$-pseudoscalar masses are input parameters for η–η' fit in Table II. The last column is the constituent quark mass $\mathcal{M}_q(0)$ pertinent to the corresponding $q\bar{q}$ meson, namely $\mathcal{M}_u(0) = \mathcal{M}_d(0)$ for the pion and $\mathcal{M}_s(0)$ for the unphysical $s\bar{s}$ pseudoscalar. The masses m_P and $\mathcal{M}_q(0)$ as well as the pseudoscalar axial-current decay constants f_P are in units of GeV, while the $\gamma\gamma$ decay amplitudes $T_P(0,0)$ are in GeV^{-1}.

	A	B	C	D	E
X	1.0	0.673	0.805		
3β	0.707	0.865	0.801		
θ	-19.5°	-11.1°	-14.9°	-12.8°	-
m_η	0.5048	0.5777	exp.		0.54730
$m_{\eta'}$	0.9809	0.9398	exp.		0.95778
$\Gamma(\eta \to \gamma\gamma)$	0.63	0.44	0.52	0.48	0.46 ± 0.04
$\Gamma(\eta' \to \gamma\gamma)$	3.61	4.61	4.16	4.41	4.26 ± 0.19

TABLE II. Various fits for the masses, mixing angle θ, and $\gamma\gamma$ decay widths Γ in the η–η' complex. In columns A, B, and C, the free parameter in the mass matrix is β, whereas X is free only in column C. Column A: results with $X = 1$ fixed by hand and β fixed by fitting $m_\eta^2 + {m'_\eta}^2$. Column B: results with X estimated from the ratio of the reduced strange and nonstrange $\gamma\gamma$ amplitudes, and β fixed by fitting $m_\eta^2 + {m'_\eta}^2$. This column gives the best predictions, especially considering its only free parameter is β. Column C: results with X treated as the second free parameter, making possible that m_η and $m_{\eta'}$ are both fitted to their experimental values exactly. Column D: fitting the empirical $\gamma\gamma$ widths of η and η' with θ as the free parameter (and empirical m_η and $m_{\eta'}$), independently of the masses and θ obtained from the mass matrix considerations. Column E: experimental values. Among the dimensionful quantities, 3β is in units of GeV^2, m_η and m'_η in GeV, while $\Gamma(\eta \to \gamma\gamma)$ and $\Gamma(\eta' \to \gamma\gamma)$ are in units of keV.

FIGURE CAPTIONS

Fig. 1: Nonperturbative QCD quark annihilation illustrated by the diagram with two-gluon exchange. It shows the transition of the $f\bar{f}$ pseudoscalar P into the pseudoscalar P' having the flavor content $f'\bar{f}'$. The dashed lines and full circles depict the $q\bar{q}$ bound-state pseudoscalars and vertices, respectively.

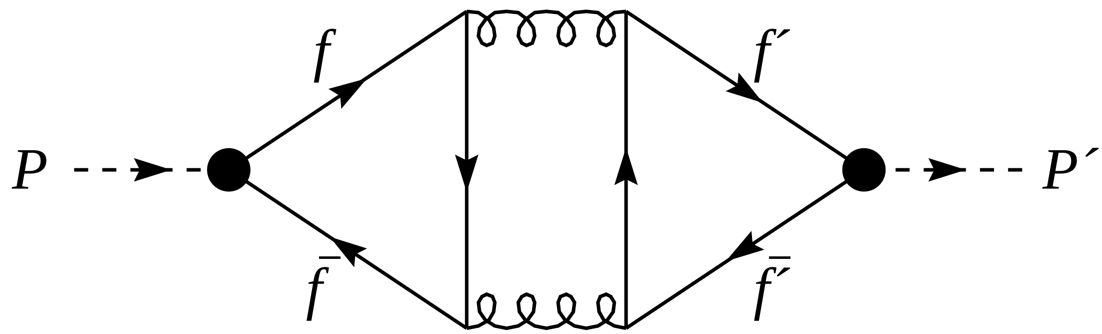
P
f
$\bar{f}$
f´
$\bar{f}$´
P´